Co-published by
Institute of Fluid-Flow Machinery
Polish Academy of Sciences
Committee on Thermodynamics and Combustion
Polish Academy of Sciences

http://www.imp.gda.pl/archives-of-thermodynamics/

An Innovative Device for Measuring Thermal Conductivity of Solids Utilising Transient Measurement Methods

M. S. Karthik[a], Mangalpady Aruna[b], P. Siva Kota Reddy[c,d]*

[a]Department of Mechanical Engineering, JSS Science and Technology University, Mysuru 570 006, Karnataka, India.
[b]Department of Mining Engineering, National Institute of Technology, Karnataka, Surathkal, Mangalore 575 025, Karnataka, India.
[c]Department of Mathematics, JSS Science and Technology University, Mysuru 570 006, Karnataka, India.
[d]Universidad Bernardo O'Higgins, Facultad de Ingeniería, Ciencia y Tecnología, Departamento de Formación y Desarrollo Científico en Ingeniería, Av. Viel 1497, Santiago, Chile.
*Corresponding author email: pskreddy@jssstuniv.in

Received: 06.21.2025; revised: 21.02.2026; accepted: 25.02.2026

Abstract

This paper presents the development of a novel experimental device for measuring the thermal conductivities of both non-conductive and conductive solids under transient conditions. The device comprises a sensor assembly coupled with an electronic bridge circuit and a direct current power source. The developed device was successfully used to measure the thermal conductivity of non-conducting and conducting solids, specifically granite and stainless steel 304, at room temperature. The device was also extended to two additional non-conducting solids, namely, limestone and basalt, to validate the testing. The thermal conductivities of granite, stainless steel-304, limestone and basalt were 2.14 W/(m·K), 14.93 W/(m·K), 2.91 W/(m·K), and 2.72 W/(m·K), respectively. These findings demonstrate excellent concordance with the existing literature for both non-conducting and conducting solid materials. The standard uncertainty of the developed device was ± 4.2%. The entire measurement process takes less than 5 s.

Keywords: Thermal conductivity; Sensor assembly; Electronic bridge circuit; Transient technique; Solids.

Vol. 47(2026), No. 1, 213–226; doi: 10.24425/ather.2026.158671

Cite this manuscript as: Karthik, M.S., Aruna, M., & Reddy, P.S.K. (2026). An Innovative Device for Measuring Thermal Conductivity of Solids Utilising Transient Measurement Methods. *Archives of Thermodynamics*, 47(1), 213−226.

1. Introduction

The ability to measure thermal conductivity is critical in determining the transfer of heat in numerous fields, including automotive, building insulation, mining, power generation, aerospace and engineering. The measurement of thermal conductivity can be accomplished through many methods, and for the majority of the methods, each method will be limited to a specific type of speed and solid and liquid materials. The thermal conductivity can be measured using experimental methods; these methods can be divided into two groups: steady-state methods (also known as continuous methods) and transient methods [1]. The principle behind steady-state devices that measure thermal conductivity is that one end of a sample is heated. At the same time, the other is cooled until equilibrium is reached, and data are collected to determine the sample's thermal conductivity (its thermal properties). However, measuring thermal conductivity with steady-state methods has drawbacks, as they require significant time for a sample to stabilise before it can be used for thermal conductivity measurements. In most laboratories where traditional devices are used to measure the thermal conductivity of solids, heat transfer must reach a steady state before experimenting, typically requiring 60 minutes. Different measuring devices are used to measure the thermal conductivities of different materials. Alterations in the sample's physical structure due to heating are an additional limitation of the steady-state approach for

Nomenclature

k – thermal conductivity, W/(m·K)
P – power input per unit length of heating wire, W/m
$T_{(t)}$ – temperature at time t, K
ΔT – temperature rise ($T_{(t2)} - T_{(t1)}$), K
t – time, s
u_k – standard uncertainty of thermal conductivity
u_m – standard uncertainty of temperature vs. ln time slope
u_p – standard uncertainty of power input

Subscripts

t_1 – initial time for measurement, s
t_2 – final time for measurement, s

Abbreviations and Acronyms

ADC – analogue-to-digital converter
ASTM – American Society for Testing and Materials
DC – direct current
GPIO – general purpose input/output
HDMI – high-definition multimedia interface
ISO – International Organization for Standardization
MOSFET– metal-oxide-semiconductor field-effect transistor
SBC – single-board computer
USB – universal serial bus

determination of the thermal conductivity. This phenomenon may influence or distort thermal conductivity measurements. Ailawalia and Priyanka [2] examined the influence of variable thermal conductivity within a semiconducting medium situated beneath an infinite elastic half-space. Leśniewski et al. [3] proposed a novel method for determining the thermal conductivity of porous ceramic materials based on the Stefan Boltzmann law of thermal radiation. Hemalatha et al. [4] used a two-slab guarded hot-plate apparatus to measure the thermal conductivities of natural fibre reinforced composites. The results from this study provided information for the future development of more sustainable materials for electrical component applications, including socket pins and switchboards. Using heat fluxes as the basis for balancing, Pistun et al. [5] developed a measurement apparatus to determine the thermal conductivity of solid materials; this apparatus uses both the steady-state technique and the bridge measurements method to determine thermal conductivity of solids. Huang and Wang [6] characterised the thermal conductance of their samples for the hotplate method by calculating the total error associated with their measurements to be ±5.2% due to uncertainty from standard techniques and also by using standard error propagation. Each test required approximately 40 minutes to reach steady-state heat transfer conditions.

1.1. Transient technique

Transient heat transfer is a critical area for many industries, including energy systems, electronics and material processing. A proper understanding of the dynamic behaviour of temperature fields within these industries contributes directly to the quality of many chemical products as well as to the reliability and safety of final manufactured goods, thus enabling more reliable estimates of future product quality. Accurate prediction of dynamic temperature processes within these types of industries also enables users to optimise their operations; therefore, prediction of temperature behaviour reduces costs associated with the production of goods. At the heart of the transient heat-transfer process is the unsteady heat conduction equation (this is a partial differential equation) derived from Fourier's law, which relates the rate of change in temperature over time (temporal) and the thermal conductivity (conductive heat) of the material being tested, as well as the temperature gradient within the material (spatial) and the time at which the temperature is measured. In contrast to steady-state collection methods, transient techniques enable rapid economical evaluation of a sample's thermal conductivity. Devices that use transient-state techniques produce a response upon introducing heat into the material over a defined time, allowing the time-dependent thermal response of the sample to be evaluated. When evaluating a sample using the transient technique, the sample does not have to reach equilibrium before a measurement can be taken. Another major reason why transient techniques are commonly used is that they offer several benefits over steady-state methods, including ease of setup, short testing times and, most importantly, low measurement uncertainty [7,8].

The transient measurement technique is ideal for measuring materials that consist of several layers or are heterogeneous materials (having multiple types of material in a single object). There are several different types of transient measurement techniques based on the mode of heat generation, temporal-based configurations of instruments and geometrical shapes (sources) of the heat source that are used. Some transient measurement techniques do not require any kind of physical interaction between the test specimen and the heating source, while other techniques require physical contact between the two. Yoon et al. [9] conducted research on the thermal conductivity of bentonite buffer materials using the hot-wire technique, and Wu et al. [10] studied the effect of natural convection on the thermal conductivity of liquids using the transitory plane source method, coupled with computational simulations to reflect the transitory heat transfer processes taking place in the liquid state.

Kosowska-Golachowska et al. [11] employed a laser flash apparatus to quantify the thermal conductivity of an array of solid fuels, i.e. brown coal, hard coal and anthracite. Mo and Ban [12] studied the thermal conductivity of particulate beds at varying levels of compressive pressure, both under air and vacuum, via a hot-disk TPS 500 instrument. Memon [13] examined the thermal conductivity of cerasolzer CS186 and J-B epoxy-steel welded resins that were used for hermetic edge sealing, through the transient method. Zheng et al. [14] evaluated 17 models used to determine the thermal conductivity of frozen soil, focusing on silty clay, sand and sandy loam, via the transient method. Asadi et al. [15] investigated the thermal conductivities of cement mortars with a transient-plane-source (TPS) device. AlQdah [16] analysed the thermal conductivities of building materials in Medina, Saudi Arabia, under natural and local environmental conditions using a specialised equipment. Liu et al. [17] developed novel instruments for pre-drilling thermal-probe testing for evaluating thermo-physical properties of soil and rock.

1.2. Transient hot-wire method

The transient hot-wire technique is among the most important techniques to measure thermal conductivity [18]. The transient hot-wire method has become one of the most common, extensively used methods to determine thermal conductivities of liquids and solids, because of its superior accuracy (low level of uncertainty), and because of its capability for absolute measurement. Furthermore, there is an extensive body of literature that documents the establishment and theoretical framework behind the use of the transient hot-wire method [19,20]. The hot-wire method consists of heating a thin metallic wire by providing an electric current to it and inserting it in a sample. The wire temperature was determined as the heat dissipated from it into the sample. The sample material's ability to conduct heat can be determined by utilising the wire temperature and the logarithm of time. One variant of the hot-wire method is known as the "probe" technique. This arrangement measures the response of a "needle" that is inserted into the material to determine the sample's thermal conductivity [21]. The test methodology and data evaluation approach of the needle probe technique were established according to the American Society for Testing and Materials (ASTM) D5930 [22] and ASTM D5334 [23]. The probe incorporated both a thermocouple and a hot-wire heater. Other techniques include the dynamic hot-wire method, which employs an embedded wire in the sample to simultaneously function as a temperature sensor and heating element [24]. Constant electric power was utilised to heat the wire during the measurement. The wire's electrical resistance as a function of temperature was used to estimate the mean temperature of the heated wire over time. The way in which a specimen responds to a temperature change is primarily unaffected by its thermal conductivity, which is why so many researchers have turned to utilising the transient hot-wire method, due to the relative simplicity of its operation, for rapid determination of a material's thermal conductivity [7,8].

Transient hot-wire techniques have also been extensively developed into a widely accepted standard for accurately determining the thermal conductivity of various types of materials: solids [24], polymeric materials [25,26], liquids [25]. In addition, it has been established that transient hot-wire measurement techniques use a Fourier-type transient conduction method to transfer heat by conduction. The first use of the transient hot-wire technique for determining the thermal conductivity of rocks began in the 1960s [26]. Over the years, investigators have developed and refined various types of instruments for the transient hot-wire method to improve the precision of transient hot-wire measurement techniques [27–33]. In the recent past, the transient hot-wire technique has been used to determine the thermal conductivity of various kinds of materials that possess low thermal conductivities [34], for example, soil [35], ice cores [36,37], biological materials [38], ceramics, and refractory materials [39]. Transient hot-wire techniques, which have been utilised to characterise other materials including glass, porous elements and powdered chemicals, have also been applied within numerous different scientific disciplines to investigate the thermal characteristics of many different kinds of materials, including biological tissues, nano-scale liquids, and composite materials comprised of both nanometre and micrometre sized features. Many different research studies have focused on determining the thermal properties of a variety of these different materials using the transient hot-wire technique [40–44]. This is possible because the transient hot-wire technique enables investigators to measure both thermal diffusivity and thermal conductivity simultaneously. Comprehensive guidelines on the hot-wire measurement technique will be provided to those interested in performing thermal conductivity determination tests on refractory materials using the hot-wire technique in accordance with ASTM C1113 and ISO 8894 [39,45].

The hot-wire technique is established under the theoretical concept of "uniaxial radial heat flow," which occurs within a uniform and consistent test material, as shown in Fig. 1.

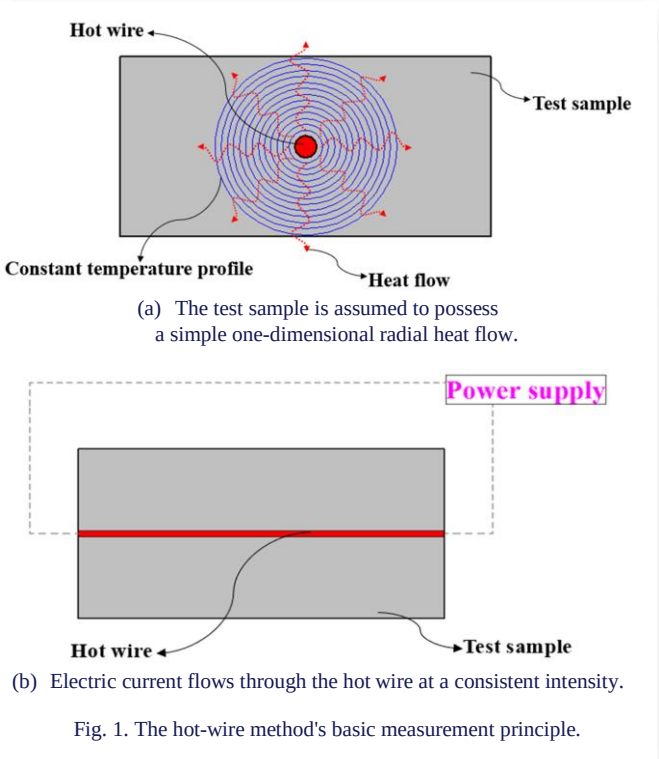

(a) The test sample is assumed to possess a simple one-dimensional radial heat flow.

(b) Electric current flows through the hot wire at a consistent intensity.

Fig. 1. The hot-wire method's basic measurement principle.

Variant (a) of Fig. 1 illustrates the test sample with an assumed simple one-dimensional radial heat flow originating from the centre of the hot-wire (sensor), creating a constant temperature profile that radiates outward radially. Variant (b) shows the electric current flowing through the hot wire embedded in the test sample at a consistent intensity (cross-sectional view). These illustrations together represent the basic measurement principle of the hot-wire method. These theoretical assumptions rely on the notion that the linear heat source is infinitely long and has a negligible diameter.

A variety of approaches to eliminating systematic errors in measurements taken under non-ideal conditions for accurately measuring the thermal conductivity of solid samples have been proposed by many researchers. Some solutions require the measurement of temperature at the end of the wire to be corrected [46,47], but these corrections tend to be smaller than those found under ideal conditions. The majority of corrections used to correct for systematic errors in hot-wire measurements relate to the effect of the heat lost from the wire due to convec-

tion and radiation. Some corrections are able to estimate the amount of heat lost through radiation by using mathematical models to determine the radiative losses, which are then applied as corrections to the temperature difference measured in the hot-wire system [48].

The objectives of the present work are as follows:

- to develop a novel device capable of measuring the thermal conductivity of both non-conductive and conductive solid samples,
- to establish a method to determine the thermal conductivity of both non-conductive and conductive solid test samples using the aforementioned device,
- to present a novel device and technique that functions under transient conditions and enables quicker measurements of thermal conductivity,
- to present a novel device and method that is accurate, cost-effective, straightforward and easily implementable.

The new thermal conductivity measurement device incorporates a unique combination of features that enable thermal conductivity measurements of both non-conductive and conductive solids. A U-shaped hot-wire configuration was incorporated into the design to increase sensitivity, flexibility and spatial resolution. To protect the hot-wire and minimise contact resistance with the sample, polyimide films were used for lamination. Additionally, a microprocessor-based electronic bridge circuit was used for improved data acquisition and processing. One of the most significant advantages of the new measurement device compared to conventional methods is that it measures the thermal conductivity of both non-conductive and conductive solids in less than 5 seconds, representing a substantial savings in measurement time. The proposed design is more efficient, more cost-effective and simpler than current technologies. However, the accuracy and precision of the new measurement device have been maintained through the use of modern electronic instrumentation. Because the exposure time of each sample is minimal, samples will not be altered due to changes in the physical structure of the sample. The device's portable design enables on-site measurement and makes it useful for a wide variety of applications. To evaluate the functionality of the new measurement device, a comparison of the thermal conductivity measurements made with the new device to literature values was performed. The results were found to be in good agreement and will be discussed in subsequent sections.

2. Experimental section

2.1. Origin of the test samples

The granite samples used in the present study were obtained from Ilakal, located in the Bagalkote district of Karnataka, India, an area renowned for its high-quality granite quarries. Limestone specimens were sourced from the Gulbarga district of Karnataka, India, which is recognised for its extensive limestone deposits. Basalt samples were collected from the Deccan Plateau region in Raichur (specifically from the Hutti gold mines area), Karnataka, India, which is characterised by widespread basaltic lava flows. Stainless steel – grade 304 (UNS S30400) was procured from AZO Materials.

2.2. Description of the experimental device

This investigation aims to use the transient dynamic hot-wire method to determine the thermal conductivity of both non-conductive and conductive solid materials. Figure 2 outlines the overall experimental workflow adopted in the present study. The procedure begins with the collection and preparation of reference samples, including non-conductive solids (granite, limestone, basalt) and a conductive solid (stainless steel 304). Concurrently, the design and development of the novel experimental setup are carried out, which involves reviewing the theoretical framework, designing the hot-wire sensor, developing the resistance sensing and heating circuit, and setting up the data acquisition system. The calibration procedure is then performed by testing the reference samples with known thermal conductivity. During the experiment, temperature changes are recorded over a defined time interval to determine thermal conductivity. If errors occur, adjustments are made by revisiting the experimental setup. Finally, the results are analysed, followed by interpretation and conclusions. The apparatus and methodology described herein adhered to the standards outlined in ISO-8894 [45] and ASTM C1113M – 09 [39].

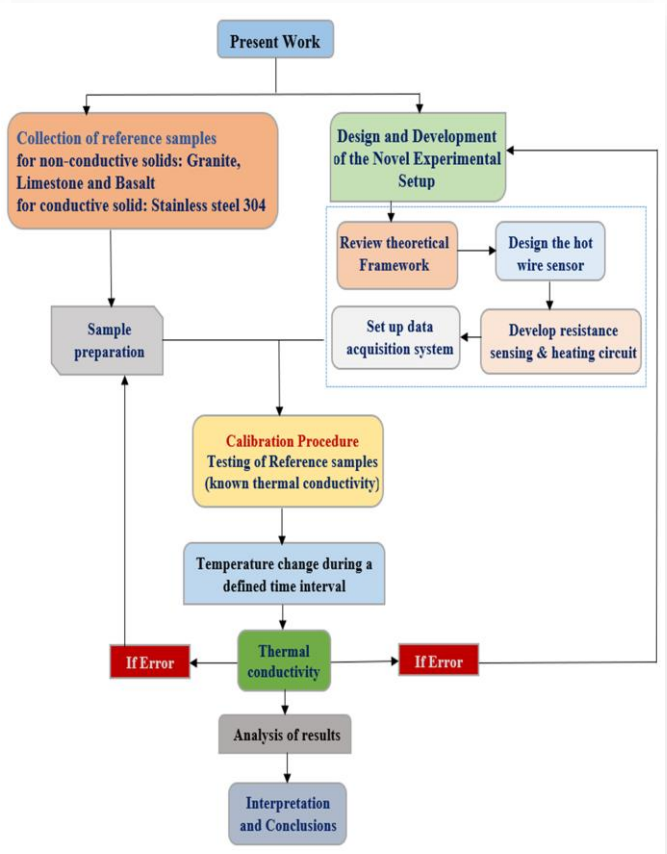

Fig. 2. Flow chart of the experimental procedure.

2.2.1. Sensor assembly

A newly developed device for measuring thermal conductivity consists of a sensor assembly, an electronic bridge circuit in electrical communication with the sensor assembly, and a direct current (DC) power source in electrical communication with the electronic bridge circuit. As shown in Fig. 3, the sensor assembly consists of a U-shaped hot-wire, a leading wire with one end spot-welded to the end of the U-shaped hot-wire, a barrel jack connection plug connected to the other end of the leading wire, and two polyimide films (Kapton) laminating the U-shaped hot-wire.

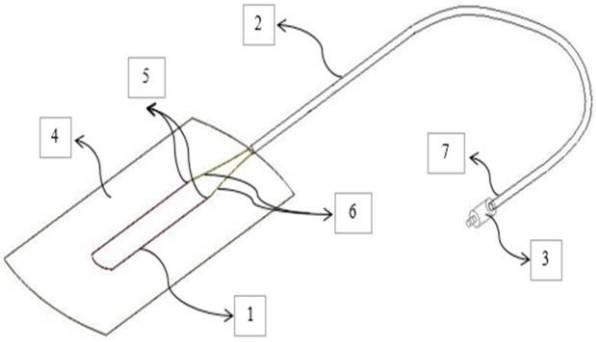

Fig. 3. Sensor assembly: 1. a U-shaped hot-wire, 2. a leading wire, 3. a barrel jack connection plug, 4. a polyimide film (Kapton), 5. an end of the U-shaped hot-wire (1), 6. an end of a leading wire connected to U-shaped hot-wire, 7. an end of a leading wire connected to barrel jack connection plug.

Figure 4 shows the geometry of the U-shaped hot-wire laminated using two polyimide films (Kapton). The U-shaped hot-wire is made up of an electrically resistive material wire of 150 µm diameter and 100 mm length. The electrically resistive material wire is platinum-rhodium wire with 90% platinum and 10% rhodium.

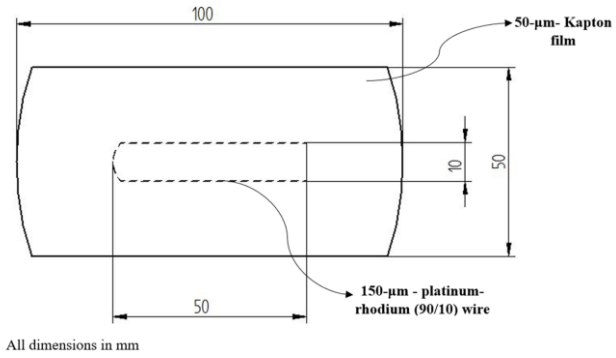

Fig. 4. Geometry of a U-shaped hot-wire laminated using two polyimide films.

The U-shaped configuration of a hot-wire must have its parallel legs separated by enough distance to decrease the heat transfer, which will increase the transfer capacity of the device while maintaining the uniformity of the radial heat flow between its legs. According to Lyu et al. [49], the spacing should be at least 6.8 times greater than the diameter of the pile, thereby ensuring that the pile-to-pile thermal interactions do not affect the radial heat flow patterns between piles. We therefore designed our U-shaped sensors with a spacing of approximately 10 mm between the parallel legs of the sensor, which is greater than the minimum needed to maintain isolated radial heat flow. In addition, Zhang and Fujii [50] found that by using insulating materials or coatings that are matched to or insulated from the heat properties of the materials they support, the radial distributions of heat flow from hot-wires can be improved. U-shaped hot-wire configurations can be effectively applied to a wide range of industrial, scientific and monitoring applications. U-shaped configurations of hot-wire sensors increase the sensors' sensitivity, flexibility and spatial resolution. Along with serving as a temperature sensor to record the increased temperature due to fluctuations in resistance, the U-shaped hot-wire also functions as a heating element when in contact with the solid test samples, establishing a temperature field that changes with time inside the solid test samples. The leading wire is a double-core and low-noise-shielded wire of 0.5 mm diameter. The leading wire serves as a support to the U-shaped hot-wire that is used as a sensor. With this arrangement, the U-shaped hot-wire that is used as a sensor is free from any kind of stress, when it is plugged or unplugged from the electrical connection. Further, laminating the U-shaped hot-wire by utilising two 25 µm thick heat-resistant sheets to protect the U-shaped hot-wire and minimise the contact resistance between the U-shaped hot-wire and the solid test sample.

2.2.2. Electronic bridge circuit

The electronic bridge circuit shown in Fig. 5 of this present work has consisted of a resistor divider circuit powered by a DC source, an analogue-to-digital converter (ADC) circuit connected to the resistor divider circuit, a metal-oxide-semiconductor field-effect transistor (MOSFET) used as a switch to control the voltage measurements across the resistor divider circuit, a transistor used to control the MOSFET switch, and a microprocessor connected to the ADC and transistor.

The resistor divider circuit, also known as a voltage divider circuit, is created by connecting the sensor assembly in series with a 0.5-ohm fixed resistor. This resistor divider circuit divides the input voltage from a continuous direct current (DC) power source into smaller voltages. The power source of direct current is used to supply power to the sensor assembly by maintaining a constant electrical current in the resistor divider circuit throughout the measurement procedure. The direct current is a regulated power source with the highest voltage and current setting a value of 30V and 2A, respectively. On drawing of current greater than the predetermined set limit by the electronic bridge circuit, the power supply of direct-current instantly transitions to the mode of constant current by lowering the voltage in a time period of the order of milliseconds after starting the process, as the load is minimal, considering 0.5-ohm resistances of the fixed resistor and resistance of the U-shaped hot-wire. Voltage data corresponding to different times at the junction point between the sensor assembly and the 0.5-ohm fixed resistor is measured using the ADC module and converted from an-

alogue to digital form. The MOSFET switch works with 5V logic, and the Raspberry Pi's general-purpose input/output (GPIO) pins can only provide 3.3V. A transistor is used to drive the MOSFET switch. The microprocessor (Raspberry Pi) via GPIO 4 drives the transistor. To turn on the transistor, a small current from the base to the emitter of the transistor is required. To limit this current, a 1-kiloohm resistor is used. The MOSFET switch is active low, which means that the MOSFET switch turns ON when the GPIO 4 is made low and turns OFF when the GPIO 4 is high. Low and high indicate the digital signals (0 and 1 in binary) whose voltage levels depend on the board used. On the Raspberry Pi microprocessor, low is 0V and high is 3.3V. The MOSFET switch requires 5V at the gate to turn it ON and 0V at the gate to turn it OFF. When GPIO 4 is high, the transistor is ON and pulls the MOSFET switch's gate terminal to 0V, turning it OFF. When GPIO 4 is low, the transistor is in OFF state, and the voltage at the gate becomes 5V because of the 10-kiloohm pull-up resistor, thus turning ON the MOSFET switch.

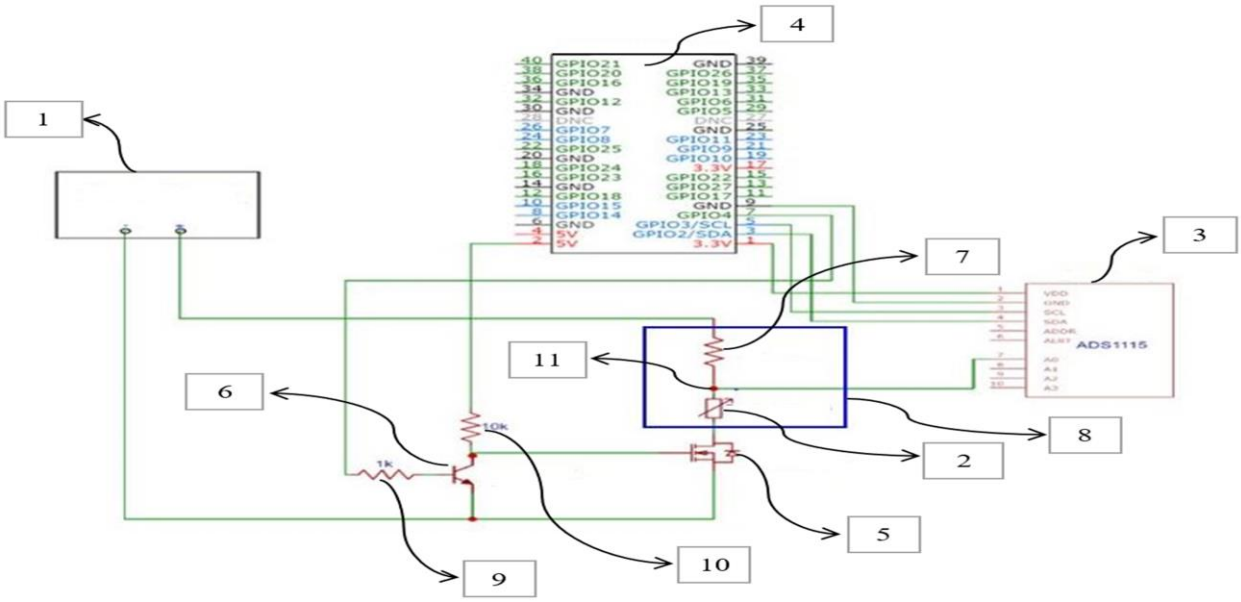

Fig. 5. Electronic bridge circuit: 1. a direct current (DC) power source, 2. a sensor assembly, 3. an analogue-to-digital converter (ADC) module, 4. a microprocessor, 5. a metal-oxide-semiconductor field-effect transistor (MOSFET) switch, 6. a transistor, 7. a 0.5-ohm fixed resistor, 8. a resistor divider circuit, 9. a 1 kiloohm resistor, 10. a pull-up resistor of 10 kiloohms, 11. a junction point of the sensor assembly (2) and the 0.5-ohm fixed resistor (7).

To keep the MOSFET switch OFF by default, a high signal is sent from GPIO 4. GPIO 4 is set to low only when the measurement is started. The microprocessor is used to convert the voltage measured with respect to time by the analogue-to-digital converter module to resistance and temperature for the calculation of thermal conductivity of solid test samples. The device operates in a transient condition, resulting in thermal conductivity measurement in a time period in a range of 1–5 seconds.

The Raspberry Pi functions as a single-board computer (SBC) equipped with a 64-bit Broadcom BCM2837 CPU featuring four cores operating at 1.2GHz and 1GB of RAM. This microprocessor utilises the Raspbian Operating System, which is stored on a 16GB SD card. The device is equipped with Universal Serial Bus (USB) and High-Definition Multimedia Interface (HDMI) ports, as well as 40 general-purpose input/output (GPIO) pins that facilitate connectivity with various hardware components. It is powered using a 5.1V 3A power adaptor. By connecting a mouse, a keyboard to the USB ports, and a monitor to the HDMI port, it can work as a small personal computer. A Python program is written on the Raspberry Pi. Figure 6 shows the flowchart for a Python program used to measure the thermal conductivity of a solid sample using an instrument as per the present work. When this program is executed, it turns on the resistor divider circuit by driving the MOSFET switch and collects the analogue data through an analogue-to-digital converter module. The final output of the code is a CSV file containing temperature-versus-time data.

By plotting temperature versus time and measuring the slope of the linear portion of the curve, the thermal conductivity of the test sample is calculated.

The thermal conductivity of the material under investigation was calculated by determining the slope of the line relating the temperature difference (ΔT) to the natural logarithm of time ($\ln t$). The temperature (T) of the U-shaped hot-wire was measured as a function of time (t), which was subsequently used to calculate the sample's thermal conductivity (k) using Eq. (1):

$$k = \frac{P}{4\pi\left(T_{(t2)} - T_{(t1)}\right)} \ln\left(\frac{t_2}{t_1}\right), \quad (1)$$

where k – thermal conductivity in W/(m·K), P – power input per unit distance along the linear heating source in W/m, $\Delta T = (T_{(t2)} - T_{(t1)})$ – temperature rise in K, and $\ln(t_2/t_1)$ – logarithm of time in seconds.

Table 1 provides a detailed description of the various components and specifications of the newly developed device for measuring the thermal conductivity of solids.

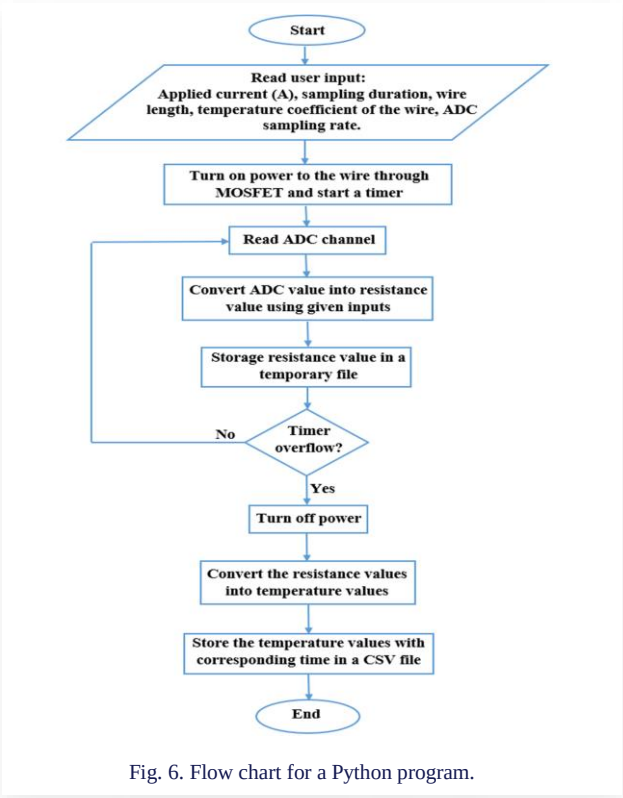

Fig. 6. Flow chart for a Python program.

3. Results and method for measuring thermal conductivity of solid samples

The device and method described in the present study are used to measure the thermal conductivity of solid test samples, including granite, stainless steel-304, limestone and basalt. The hot-wire sensor size cannot exceed the accessible sample size, as required by transient methods. Notably, each solid test sample should have a minimum thickness of 5 mm, a length of 100 mm, and a breadth of 50 mm, according to the U-shaped sensor's design requirements.

Several strategies can be employed to minimise the thermal contact resistance at the U-shaped sensor-solid sample interface. Optimising surface preparation is essential to ensure that sample surfaces are smooth, flat and thoroughly cleaned, thereby eliminating contaminants. Furthermore, in applications requiring a reduction in the contact resistance of electronic devices, the structural integrity and thermal stability of Kapton render it a preferred choice [51]. For instance, Romero et al. [52] focused on the laser ablation of Kapton polyimide, which demonstrated promising electrical and thermal characteristics, indicating its potential as a flexible, conductive substrate. The use of polyimide films (Kapton) is based on creating a uniform and conformal interface between the sensor and sample, which reduces the

Table 1. Components and specifications of the instrument as per the present work.

No.	Components	Specifications
1	U-shaped hot-wire	Platinum-rhodium with 90% platinum and 10% rhodium, diameter =150 µm , length = 100 mm
2	Leading wire	Double-core, low-noise-shielded wire, diameter = 0.5 mm
3	Connection plug	DC barrel jack plug
4	Polyimide film	Kapton, thickness = 25 µm + 25 µm = 50 µm
5	Power source	Maximum – 30 V and 2 A, DC power supply
6	analogue-to-digital converter (ADC) module	ADC - ADS1115, 16-bit conversion, maximum data rate of 860 samples per second
7	Microprocessor	The Raspberry Pi incorporates a 64-bit CPU, specifically, a Broadcom BCM2837 Quad Core processor operating at 1.2GHz. It is equipped with 1GB of RAM and includes a 16GB SD card for data storage purposes.
8	MOSFET switch	IRFZ44N – drain current DC = 49 A (maximum), drain source voltage = 55 V (maximum), drain-source on-resistance = 22 mΩ (maximum), fast switching
9	Transistor	2N3904, emitter - 40V(maximum), base – 60 V (maximum), collector current - 200 mA
10	Fixed resistor	0.5 Ω, 3 W
11	Resistor	1 kΩ
12	Pull-up resistor	10 kΩ

gaps and imperfections that typically contribute to increased contact resistance. In the present work, the U-shaped hot-wire laminated with two polyimide films (Kapton) is squeezed between two solid test samples to measure its material's thermal conductivity.

Empirical models and experimental observations indicate that the contact resistance decreases nonlinearly with increasing compression pressure. When pressure is applied, it deforms the asperities at the contacting interface, effectively increasing the real contact area, which in turn reduces the resistance to heat flow [53,54]. This effect is crucial in applications where minimising the thermal contact resistance is necessary for efficient thermal management [55]. In our studies, to apply a minimal force on the surfaces, a metallic mass of 2 kg was mounted on top of the sample. As a result, heat is transferred to the solid test samples from the U-shaped hot-wire via the polyimide films. This methodology effectively mitigated the thermal contact resistance, enabling the apparatus to function with minimal uncertainty. This technique has proven successful in reducing contact resistance in studies involving materials such as granite, stainless steel-304, limestone, and basalt.

An arrangement of the device, as per the present work for measuring the thermal conductivity of a solid test sample, including a U-shaped hot-wire, two polyimide films, two solid test samples, and a metallic weight used to test the thermal conductivity at the surrounding temperature, is illustrated in Fig. 7.

Figure 8 is a photograph showing the arrangement of a device as used in the present work, positioned between solid test samples, with a weight applied for the measurement of thermal conductivity.

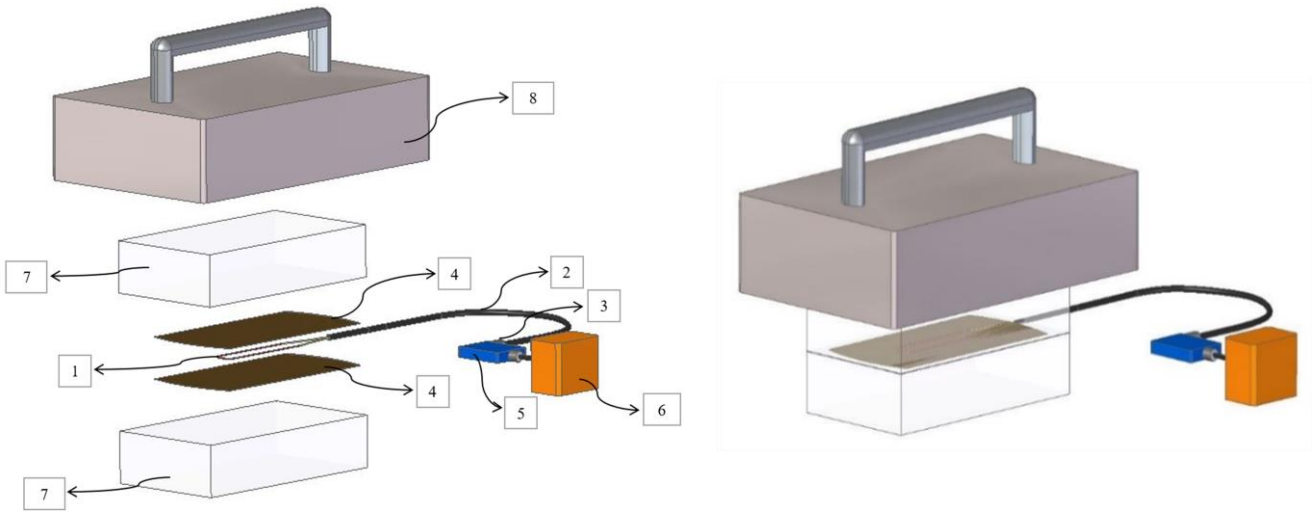

a) Exploded view b) Isometric view

Fig. 7. Arrangement of a device for measuring thermal conductivity of a solid test sample: 1. a U-shaped hot-wire, 2. a leading wire, 3. a barrel jack connection plug, 4. a heat-resistant Kapton sheet, 5. an electronic bridge circuit, 6. a direct current (DC) power source, 7. a solid test sample, 8. a metallic weight.

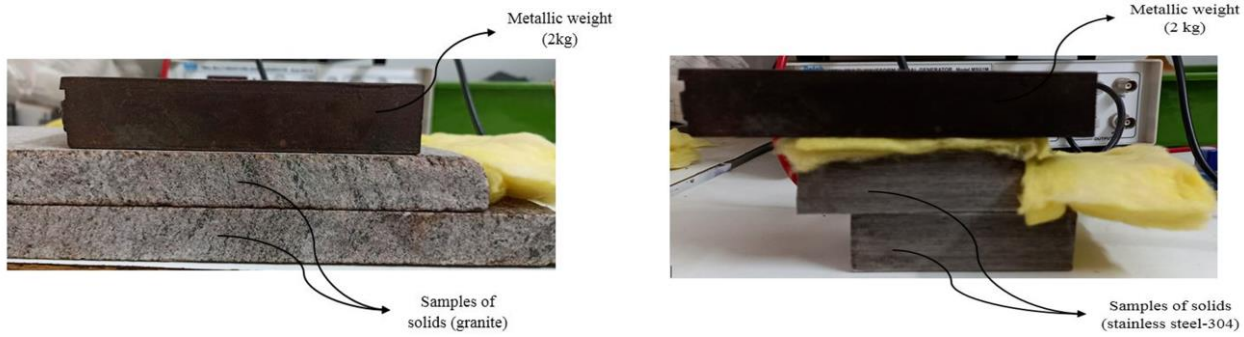

a) Granite b) Stainless steel-304

Fig. 8. Photograph showing an arrangement of the instrument with application of weight for measurement of thermal conductivity.

According to experimental findings by the instrument as per present work, a heat pulse of about 5 seconds that the U-shaped hot-wire transfers through the polyimide film (Kapton) to the solid test samples appears to be adequate to produce a temperature increase between the time t_1 and t_2 at a power (P) input of about 3 W. Total 1500 measurements are used for this run, ranging from 0 to 5 seconds.

The transient hot-wire measurement method comprises three steps. Initially, experimental resistance measurements are obtained from a U-shaped hot-wire over a specified time period. Subsequently, the temperature was derived from these data. Over time, the temperature of the U-shaped hot-wire exhibited a logarithmic pattern. Therefore, when plotting the temperature against time on a semi-logarithmic graph to measure the thermal conductivity via the transient hot-wire method, it is standard practice to exclude the initial segment of the temperature versus time data points [44]. Hence, we focus our analysis on the upper linear portion of the plot. This methodology is essential for achieving precise thermal conductivity measurements and involves several critical factors. The initial segment of the temperature-time plot frequently exhibits transient effects that are inconsistent with the steady-state heat conduction model. During this phase, the temperature increase may be influenced by thermal inertia and other transient phenomena, potentially distorting the measurements [44]. The upper linear portion of the plot indicates the establishment of a quasi-steady state condition or thermal equilibrium, where the temperature increase follows a predictable and consistent pattern. This linear behaviour signifies that the system has reached a state in which the assumptions of the transient hot-wire model are applicable. At this point, the thermal conductivity can be accurately determined from the slope of the line [44]. By concentrating on the linear portion, the effects of noise and irregularities present in the initial transient phase can be avoided, thereby enhancing the precision of the measurement, as data points from the steady linear portion are less susceptible to such disturbances. The semi-logarithmic scale facilitates the clear identification of the linear region, simplifying the extraction of thermal properties by converting the exponential temperature increase into a linear relationship. This transformation is crucial for correlating the measured temperature increase with the theoretical model, enabling the calculation of the thermal conductivity and diffusivity [44]. These practices collectively ensure that the data used for calculating the thermal conductivity are derived from a range in which the heat transfer

mechanisms are well understood and accurately represented by the theoretical models employed in the analysis. Discarding the initial portion and focusing on the linear part mitigated errors and enhanced the reliability of the thermal conductivity measurements.

The upper linear segment is selected based on the premise that, during this phase, the temperature increase of the wire demonstrates a direct linear correlation with the natural logarithm of the time. This correlation is attributed to the predominance of heat conduction during this phase, with negligible influence from other effects, such as natural convection. The linear region was identified by ensuring that the plotted points formed a straight line with minimal deviation, thereby confirming that the conditions were primarily due to pure conduction [56]. It is advantageous if the R-squared value of the linear fit approaches 1, indicating a robust linear relationship, and if the selected region produces consistent results across multiple measurements of the same sample.

A typical experimental semi-logarithmic temperature vs. time response and its logarithmic fit for the linear portion of the experimental data for the solid test samples of granite and stainless steel 304 at the surrounding temperature are illustrated in Figs. 9 and 10, respectively. The thermal conductivity of granite and stainless steel 304 is near the upper end of the linear curve. For granite and stainless steel-304, the thermal conductivity values computed from the temperature against the time curve in a semi-logarithmic plot are 2.14 W/(m·K) and 14.93 W/(m·K), respectively. These values differ by –0.04 for granite and +0.01 to +0.59 for stainless steel 304 from the values suggested by the literature [57–60].

Tables 2 and 3 present an assessment of the measured thermal conductivity values for the granite and stainless steel-304 test samples, including their deviations, relative to the values recommended in the existing literature [57–60].

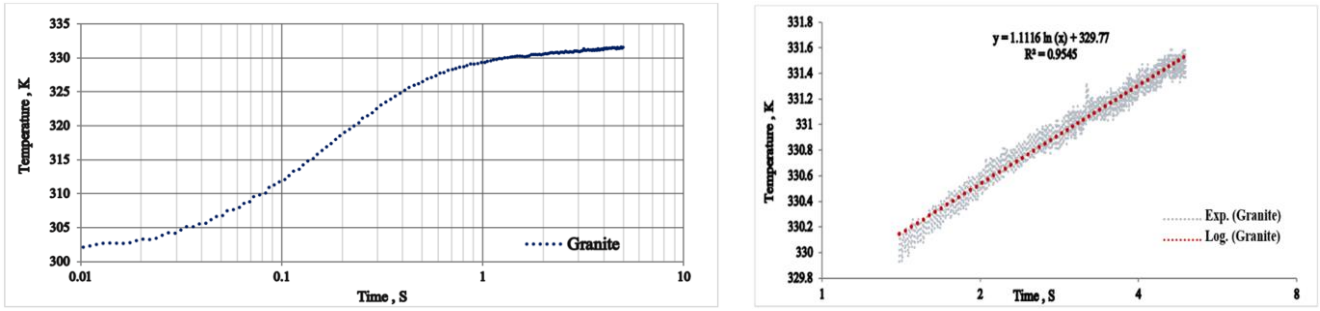

a) b)

Fig. 9. (a) Experimental temperature variation of granite with time, and (b) its logarithmic fit for the linear portion of the experimental data.

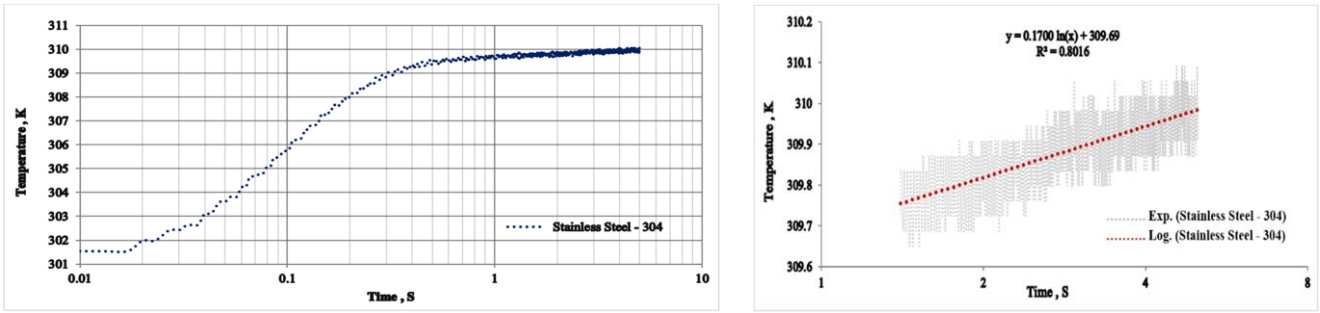

a) b)

Fig. 10. (a) Experimental temperature variation of stainless steel-304 with time, and (b) its logarithmic fit for the linear portion of the experimental data.

Table 2. Assessment of the granite samples measured thermal conductivity values, including their deviations, in relation to the value proposed in [57].

Non-conductive solid sample – granite			
Trial no.	Measured thermal conductivity at 300 K (W/(m·K))	Thermal conductivity at 300 K (W/(m·K)) [57]	Deviation
1	2.14	2.18	–0.04
2	2.16		
3	2.13		
Mean	2.14		
Standard deviation	0.016	–	
Random error in measurements (from repeated measurements) (%)	0.75%		

Table 3. Assessment of the stainless steel-304 samples measured thermal conductivity values, including their deviations, in relation to the values proposed in the literature ([58−60]).

Conductive solid sample – stainless steel-304					
Trial no.	Measured thermal conductivity at 300 K (W/(m·K))	Thermal conductivity at 300 K (W/(m·K)) [58]	Thermal conductivity at 300 K (W/(m·K)) [59]	Thermal conductivity at 300 K (W/(m·K)) [60]	Deviations
1	14.94	14.92	14.84	14.34	+0.01 [58] +0.09 [59] +0.59 [60]
2	14.93				
3	14.91				
Mean	14.93				
Standard deviation	0.016	–			
Random error in measurements (from repeated measurements) (%)	0.11%				

To assess the broad applicability of the developed device, it is essential to incorporate various solid samples. By evaluating the device across different solid samples, we can determine its performance in various contexts and identify any limitations or areas for enhancement. The thermal conductivities of solid samples, such as limestone and basalt, were examined in this study. Figures 11 and 12 present semi-logarithmic graphs illustrating the correlations between the temperature and time for limestone and basalt. These findings were obtained at ambient temperature using the apparatus developed in this study. The thermal conductivities of limestone and basalt, as determined from the semi-logarithmic temperature-time graphs, were 2.91 W/(m·K) and 2.72 W/(m·K), respectively. These results showed deviations from the literature values, with −0.06 for limestone and +0.04 for basalt, respectively [61,62].

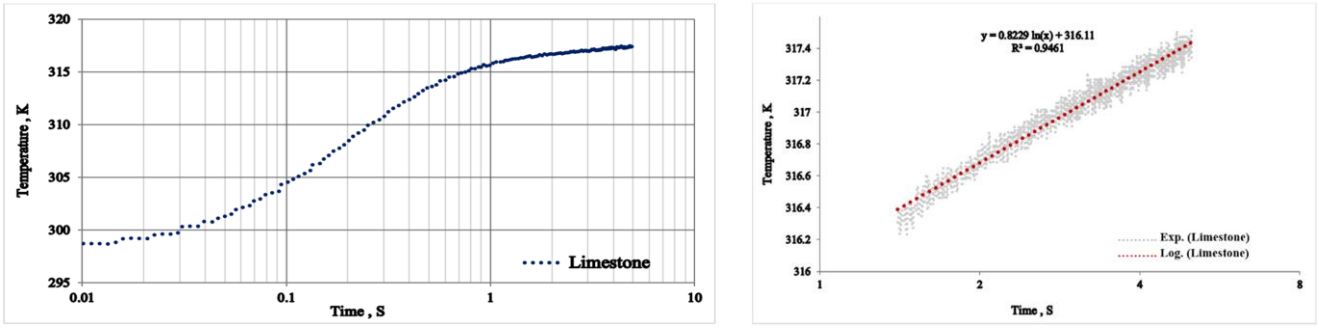

b) b)

Fig. 11(a) Experimental temperature variation of limestone with time, and (b) its logarithmic fit for the linear portion of the experimental data.

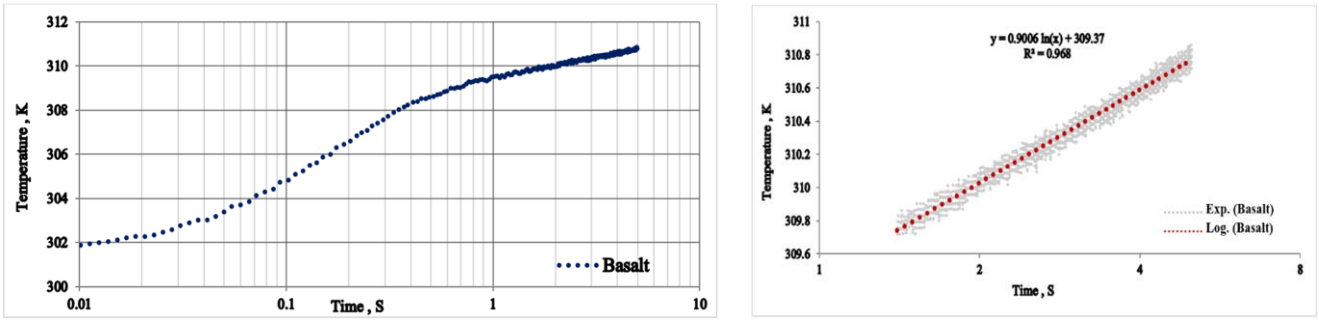

c) b)

Fig. 12. (a) Experimental temperature variation of basalt with time, and (b) its logarithmic fit for the linear portion of the experimental data.

Tables 4 and 5 provide an evaluation of the measured thermal conductivities and their deviations for the test samples using the developed apparatus, in comparison with the literature values [61,62].

This novel apparatus and methodology are appropriate for determining the thermal conductivities of both non-conductive and conductive solid materials under transient conditions. The measurement process required only 5s, facilitating a more rapid assessment than existing technologies. Moreover, this innovative approach provides a straightforward, efficient and cost-effective alternative to current methods.

Table 4. Assessment of the limestone samples measured thermal conductivity values, including their deviations, in relation to the value proposed in [61].

Non-conductive solid sample – limestone			
Trial no.	Measured thermal conductivity at 300 K (W/(m·K))	Thermal conductivity at 300 K (W/(m·K)) [61]	Deviations
1	2.89	2.97	–0.06
2	2.92		
3	2.93		
Mean	2.91		
Standard deviation	0.021	–	
Random error in measurements (from repeated measurements) (%)	0.72%		

Table 5. Assessment of the basalt samples measured thermal conductivity values, including their deviations, in relation to the value proposed in [62].

Non-conductive solid sample – basalt			
Trial no.	Measured thermal conductivity at 300 K (W/(m·K))	Thermal conductivity at 300 K (W/(m·K)) [62]	Deviations
1	2.69	2.68	+ 0.04
2	2.73		
3	2.74		
Mean	2.72		
Standard deviation	0.03	–	
Random error in measurements (from repeated measurements) (%)	1.10%		

3.1. Uncertainty analysis

The guide to the expression of uncertainty in measurement, a standard for estimating uncertainty published by the International Organisation for Standardisation (ISO) was used [63]. The contributions of the components to the standard uncertainty can be represented by the following Eq. (2):

$$u_k = \sqrt{\left(\frac{\partial k}{\partial P}\, u_P\right)^2 + \left(\frac{\partial k}{\partial m}\, u_m\right)^2}. \quad (2)$$

The standard uncertainty of the thermal conductivity is represented by u_k, where u_p and u_m denote the standard uncertainties of the power input per unit distance along the linear heating source and the slope of temperature rise versus logarithmic time, respectively.

In the present work, the uncertainty associated with the measurement of the thermal conductivity was evaluated as follows: the voltage applied to the voltage divider circuit, along with its variation during a transient experimental run, was monitored using a digital high-resolution multimeter with an uncertainty of ±1 μV. The uncertainty related to the power input per unit length of the platinum-rhodium wire (composed of 90% platinum and 10% rhodium) was assessed as ±0.2%. The temperature coefficient of the thin platinum-rhodium wire resistance was determined through calibration conducted during the measurement process, with an estimated uncertainty of ±0.2%. The experimental time was measured and recorded using an ADC (ADS1115) with a 16-bit conversion, a maximum data rate of 860 samples per second, and an uncertainty of ±1 μs. The slope of the temperature increase to the natural logarithmic time ratio was measured with an uncertainty of ±3.8%, as estimated by deviations from linearity. The experimental sensor was designed such that the thickness of the Kapton heat-resistant sheets was precisely defined and equal to 50μm, ensuring that it did not affect the uncertainty of the technique. The standard uncertainty of the developed device was assessed at ±4.2% for the measurement of the thermal conductivity of solids.

4. Conclusions

The development of novel devices based on the transient technique has been necessitated by the demand for information regarding the ability to conduct heat in both non-conductive and conductive solid test samples, and to analyse heat transfer in engineering applications without resorting to time-consuming laboratory tests. The developed apparatus exhibits multiple advantages over existing instruments, including operational simplicity and cost effectiveness alternative to current methods. The capability to evaluate thermal conductivity in both non-conductive and conductive solid specimens, with exceptional precision and accuracy facilitated by contemporary electronic instrumentation, and minimal sample exposure time is demonstrated.

The present study uses a newly developed portable instrument to analyse the thermal conductivity of both non-conductive and conductive solid test samples, such as granite, stainless steel-304, limestone and basalt, at room temperature. The transient technique applied to solid test samples yielded results that closely matched previously published data. The measured thermal conductivities were 2.14 W/(m·K), 14.93 W/(m·K), 2.91 W/(m·K) and 2.72 W/(m·K) for granite, stainless steel 304, limestone and basalt, respectively. The standard uncertainty of the developed instrument was ±4.2%. The results strongly align with existing literature. Notably, the measurement process takes around 5 seconds for solid test samples. It is realisable to employ the developed device to determine the thermal conductivity of non-conductive and conductive solid test samples, as evidenced

by the excellent agreement between experimental results and suggested data.

The future scope of this study includes several potential research directions. These studies involve exploring various wire materials and geometries to optimise the sensor performance and expand the range of measurable solids. Extending the measurement capabilities to encompass a broader range of temperatures and pressures could enhance the applicability of the device across diverse industrial settings.

Acknowledgements

The authors extend their sincere appreciation to JSS Science and Technology University in Mysore, Karnataka, India, and the National Institute of Technology in Surathkal, Karnataka, India, for providing the essential facilities required to conduct this research.

References

[1] Paul, G., Chopkar, M., Manna, I., & Das, P.K. (2010). Techniques for measuring the thermal conductivity of nanofluids: A review. *Renewable and Sustainable Energy Reviews*, 14(7), 1913–1924. doi 10.1016/j.rser.2010.03.017

[2] Ailawalia, P., & Priyanka, P. (2024). Effect of variable thermal conductivity in semiconducting medium underlying an elastic half-space. *Archives of Thermodynamics*, 45(3), 159–166. doi: 10.24425/ather.2024.151226

[3] Leśniewski, W., Czekaj, E., Wieliczko, P., & Wawrylak, M. (2019). Novel method of thermal conductivity measurement using Stefan-Boltzmann law. *Archives of Metallurgy and Materials*, 64(1), 311–315. doi: 10.24425/amm.2019.126253

[4] Hemalatha, C.K., Venkatachalam, G., & Bhuvaneshwari, M. (2025). Investigation of thermal conductivity of Prosopis juliflora/Acacia leucophloea/Acacia nilotica fibers/ceramic fillers/epoxy composites. *Results in Engineering*, 25, 104225. doi: 10.1016/j.rineng.2025.104225

[5] Pistun, Y., Matiko, H., Vasylkivskyi, I., Fedynets, V., & Krykh, H. (2024). Automated system for measuring thermal conductivity of solid materials. *Metrology and Measurement Systems*, 31(1), 179−193. doi: 10.24425/mms.2024.148538

[6] Huang, J.S., & Wang, C.Y. (2025). Numerical simulation and measurement of effective thermal conductivity of an additively manufactured lattice microstructure with gradient porosity. *Results in Engineering*, 25, 104177. doi: 10.1016/j.rineng.2025.104177

[7] Komini Babu, S., Praveen, K.S., Raja, B., & Damodharan, P. (2013). Measurement of thermal conductivity of fluid using single and dual wire transient techniques. *Measurement*, 46(8), 2746–2752. doi: 10.1016/j.measurement.2013.05.017

[8] Hong, S. W., Kang, Y.T., Kleinstreuer, C., & Koo, J. (2011). Impact analysis of natural convection on thermal conductivity measurements of nanofluids using the transient hot-wire method. *International Journal of Heat and Mass Transfer*, 54(15–16), 3448–3456. doi: 10.1016/j.ijheatmasstransfer.2011.03.041

[9] Yoon, S., Lee, G.J., Park, T.J., Lee, C., & Cho, D.K. (2022). Thermal conductivity evaluation for bentonite buffer materials under elevated temperature conditions. *Case Studies in Thermal Engineering*, 30, 101792. doi: 10.1016/j.csite.2022.101792

[10] Wu, K.F., Cao, T.F., Li, W.B., Zhang, H., & Tang, G.H. (2023). Quantitative evaluation of the natural convection effect on thermal conductivity measurement with transient plane source method. *Case Studies in Thermal Engineering*, 45, 102933. doi: 10.1016/j.csite.2023.102933

[11] Kosowska-Golachowska, M., Musiał, T., & Gajewski, W. (2014). Determination of the effective thermal conductivity of solid fuels by the laser flash method. *Archives of Thermodynamics*, 35(3), 3–16. doi: 10.2478/aoter-2014-0018

[12] Mo, J., & Ban, H. (2017). Measurements and theoretical modeling of effective thermal conductivity of particle beds under compression in air and vacuum. *Case Studies in Thermal Engineering*, 10, 423–433. doi: 10.1016/j.csite.2017.10.001

[13] Memon, S. (2017). Experimental measurement of hermetic edge seal's thermal conductivity for the thermal transmittance prediction of triple vacuum glazing. *Case Studies in Thermal Engineering*, 10, 169–178. doi: 10.1016/j.csite.2017.06.002

[14] Zheng, S.F., Wang, M., Li, X., Tai, B.W., Li, G.Y., & Mao, Z.Y. (2024). Evaluation of 17 thermal conductivity models for frozen soil. *Case Studies in Thermal Engineering*, 61, 104949. doi: 10.1016/j.csite.2024.104949

[15] Asadi, I., Ji, G., & Baghban, M.H. (2023). Evaluating the effective thermal conductivity of cement mortar through x-ray scanning. *Case Studies in Thermal Engineering*, 41, 102686. doi: 10.1016/j.csite.2022.102686

[16] AlQdah, K.S. (2021). Effect of using natural and local environment contents on the thermal conductivity of building materials: Case in Medina, Saudi Arabia. *Case Studies in Thermal Engineering*, 28, 101597. doi: 10.1016/j.csite.2021.101597

[17] Liu, Y., Mei, X., Wang, W., Zhang, G., & Cheng, W. (2023). Development and application of a novel pre-drilling thermal probe in-situ testing equipment. *Case Studies in Thermal Engineering*, 42, 102743. doi: 10.1016/j.csite.2023.102743

[18] Carslaw, H.S., & Jaeger, J.C. (1959). *Conduction of heat in solids* (2nd ed.). Oxford University Press, USA.

[19] Assael, M.J., Nieto de Castro, C.A., Roder, H.M., & Wakeham, W.A. (1991). Transient methods for thermal conductivity (Chapter 7). In *Experimental Thermodynamics. Vol. III: Measurement of the Transport Properties of Fluids* (Eds. Nagashima A., Sengers G.V., Wakeham W.A.), pp. 161 – 195. Blackwell Scientific Publications.

[20] Assael, M.J., Antoniadis, K.D., & Wakeham, W.A. (2010). Historical evolution of the transient hot-wire technique. *International Journal of Thermophysics*, 31(6), 1051–1072. doi: 10.1007/s10765-010-0814-9

[21] Tong, X. C. (2011). *Advanced materials for thermal management of electronic packaging*. Springer Series in Advanced Microelectronics, 30. Springer, New York. doi: 10.1007/978-1-4419-7759-5

[22] American Society for Testing and Materials. (1997). *Standard test method for determination of thermal conductivity plastics by means of a transient line-source technique (ASTM D5930−97)*. doi: 10.1520/D5930-97

[23] American Society for Testing and Materials. (2014). *Standard test method for determination of thermal conductivity of soil and soft rock by thermal needle probe procedure (ASTM D5334−14)*. doi: 10.1520/D5334-14

[24] Assael, M.J., Antoniadis, K.D., Metaxa, I., Mylona, S.K., Assael, Y., Wu, J., & Hu, M. (2015). A novel portable absolute transient hot-wire instrument for the measurement of the thermal conductivity of solids. *International Journal of Thermophysics*, 36(10−11), 3083–3105. doi: 10.1007/s10765-015-1964-6

[25] Nakamura, S., Hibiya, T., & Yamamoto, F. (1988). Measurement of the thermal conductivity of molten semiconductors. *International Journal of Thermophysics*, 9(6), 933–940. doi: 10.1007/BF01133261

[26] Jaeger, J.C., & Sass, J.H. (1964). A line source method for measuring the thermal conductivity and diffusivity of cylindrical specimens of rock and other poor conductors. *British Journal of Applied Physics*, 15(10), 1187–1194. doi: 10.1088/0508-3443/15/10/307

[27] Richard, R.G., & Shankland, I.R. (1989). A transient hot-wire method for measuring the thermal conductivity of gases and liquids. *International Journal of Thermophysics*, 10(3), 673–686. doi: 10.1007/BF00507988

[28] Nagasaka, Y., & Nagashima, A. (1981). Absolute measurement of the thermal conductivity of electrically conducting liquids by the transient hot-wire method. *Journal of Physics E: Scientific Instruments*, 14(12), 1435. doi: 10.1088/0022-3735/14/12/020

[29] Bleazard, J.G., & Teja, A.S. (1995). Thermal conductivity of electrically conducting liquids by the transient hot-wire method. *Journal of Chemical Engineering Data*, 40(4), 732–737. doi: 10.1021/je00020a003

[30] Roder, H.M. (1981). Transient hot wire thermal conductivity apparatus for fluids. *Journal of Research of the National Bureau of Standards*, 86, 457–493. doi: 10.6028/jres.086.020

[31] Perkins, R.A., Roder, H.M., & Nieto de Castro, C.A. (1991). High-temperature transient hot-wire thermal conductivity apparatus for fluids. *Journal of Research of the National Institute of Standards and Technology*, 96(3), 247–269. doi: 10.6028/jres.096.014

[32] Roder, H.M., Perkins, R.A., Laesecke, A., & Nieto De Castro, C.A. (2000). Absolute steady-state thermal conductivity measurements by use of a transient hot-wire system. *Journal of Research of the National Institute of Standards and Technology*, 105(2), 221–253. doi: org/10.6028/jres.105.028

[33] Johns, A.I., Scott, A.C., Watson, J.T.R., Ferguson, D., & Clifford, A.A. (1988). Measurement of the thermal conductivity of gases by the transient hot-wire method. *Philosophical Transactions of the Royal Society of London. Series A, Mathematical and Physical Sciences*, 325(1585), 295–356. doi: 10.1098/rsta.1988.0054

[34] Vozár, L. (1996). A computer-controlled apparatus for thermal conductivity measurement by the transient hot wire method. *Journal of Thermal Analysis*, 46(2), 495–505. doi: 10.1007/BF02135027

[35] Abu-Hamdeh, N.H., Khdair, A.I., & Reeder, R.C. (2000). A comparison of two methods used to evaluate thermal conductivity for some soils. *International Journal of Heat and Mass Transfer*, 44(5), 1073–1078. doi: 10.1016/s0017-9310(00)00144-7

[36] Festa, C., & Rossi, A. (1999). Apparatus for routine measurements of the thermal conductivity of ice cores. *Annals of Glaciology*, 29, 151–154. doi: 10.3189/172756499781821210

[37] Festa, C., & Rossi, A. (1997). Thermal conductivity measurement (TCM) of ice cores: Devices and procedures. *Geografia Fisica e Dinamica Quaternaria*, 20(2), 263–267.

[38] Liang, X.G., Zhang, Y., & Ge, X. (1999). The measurement of thermal conductivities of solid fruits and vegetables. *Measurement Science and Technology*, 10(7). doi: 10.1088/0957-0233/10/7/402

[39] ASTM International. (2009). *Standard test method for determination of thermal conductivity of refractories by hot wire (platinum resistance thermometer technique) (ASTM C1113/C1113M−09)*. doi: 10.1520/C1113_C1113M-09

[40] Murshed, S.M.S., Leong, K.C., & Yang, C. (2005). Enhanced thermal conductivity of TiO2-water based nanofluids. *International Journal of Thermal Sciences*, 44(4), 367–373. doi: 10.1016/j.ijthermalsci.2004.12.005

[41] Hu, Y.S., Xu, Y.S., Sun, D.A., Chen, B., & Zeng, Z.T. (2021). Temperature dependence of thermal conductivity of granular bentonites. *Yantu Lixue/Rock and Soil Mechanics*, 42(7), 1774–1782. doi: 10.16285/j.rsm.2020.1899

[42] Dos Santos, W.N., & Gregorio, R. (2002). Hot-wire parallel technique: A new method for simultaneous determination of thermal properties of polymers. *Journal of Applied Polymer Science*, 85(8), 1779–1786. doi: 10.1002/app.10681

[43] Murshed, S.M.S., Leong, K.C., & Yang, C. (2006). Determination of the effective thermal diffusivity of nanofluids by the double hot-wire technique. *Journal of Physics D: Applied Physics*, 39(24), 5316–5322. doi: 10.1088/0022-3727/39/24/033

[44] Xie, H., Gu, H., Fujii, M., & Zhang, X. (2006). Short hot wire technique for measuring thermal conductivity and thermal diffusivity of various materials. *Measurement Science and Technology*, 17(1), 208–214. doi: 10.1088/0957-0233/17/1/032

[45] International Organization for Standardization. (2010). *Refractory materials – Determination of thermal conductivity Part 1: Hot-wire (cross-array) and resistance thermometer methods*. ISO/DIS 8894-1 (pp. 1–17).

[46] Healy, J.J., & De Groot, J.J. (1976). The theory of the transient hot-wire method for measuring thermal conductivity. *Physica B+C*, 82(2), 392–408. doi: 10.1016/0378-4363(76)90203-5

[47] De Groot, J.J., Kestin, J., & Sookiazian, H. (1974). Instrument to measure the thermal conductivity of gases. *Physica*, 75(3), 454–482. doi: 10.1016/0031-8914(74)90341-3

[48] Daouas, N., Fguiri, A., & Radhouani, M.S. (2008). Solution of a coupled inverse heat conduction-radiation problem for the study of radiation effects on the transient hot wire measurements. *Experimental Thermal and Fluid Science*, 32(8), 1766–1778. doi: 10.1016/j.expthermflusci.2008.04.003

[49] Lyu, W., Pu, H., & Chen, J.N. (2020). Thermal performance of an energy pile group with a deeply penetrating u-shaped heat exchanger. *Energies*, 13(21), 5822. doi: 10.3390/en13215822

[50] Zhang, X., & Fujii, M. (2000). Simultaneous measurements of the thermal conductivity and thermal diffusivity of molten salts with a transient short-hot-wire method. *International Journal of Thermophysics*, 21(1), 71–84. doi: 10.1023/A:1006604820755

[51] Xie, Z., Dou, Z., Wu, D., Zeng, X., Feng, Y., Tian, Y., Fu, Q., & Wu, K. (2023). Joint-inspired liquid and thermal conductive interface for designing thermal interface materials with high solid filling yet excellent thixotropy. *Advanced Functional Materials*, 33(14), 2214071. doi: 10.1002/adfm.202214071

[52] Romero, F.J., Castillo, A.S., Rivadeneyra, A., Albrecht, A., Godoy, A., Morales, D.P., & Rodriguez, N. (2018). In-depth study of laser diode ablation of Kapton polyimide for flexible conductive substrates. *Nanomaterials*, 8(7), 517. doi: 10.3390/nano8070517

[53] Nitta, I., Himanen, O., & Mikkola, M. (2008). Thermal conductivity and contact resistance of compressed gas diffusion layer of PEM fuel cell. *Fuel Cells*, 8(2), 111–119. doi: 10.1002/fuce.200700054

[54] Babu, S.S., Santella, M.L., Feng, Z., Riemer, B.W., & Cohron, J.W. (2001). Empirical model of effects of pressure and temperature on electrical contact resistance of metals. *Science and Technology of Welding and Joining*, 6(3), 126–132. doi: 10.1179/136217101101538631

[55] Pan, X., Cui, X., Liu, S., Jiang, Z., Wu, Y., & Chen, Z. (2020). Research progress of thermal contact resistance. *Journal of Low Temperature Physics*, 201, 213–253. doi: 10.1007/s10909-020-02497-0

[56] Glatzmaier, G.C., & Ramirez, W.F. (1985). Simultaneous measurement of the thermal conductivity and thermal diffusivity of unconsolidated materials by the transient hot wire method. *Review of Scientific Instruments*, 56(7), 1394–1398. doi: 10.1063/1.1138491

[57] Chen, C., Zhu, C., Zhang, B., Tang, B., Li, K., Li, W., & Fu, X. (2021). Effect of Temperature on the Thermal Conductivity of Rocks and its Implication for In Situ Correction. *Geofluids*, 6630236. doi: 10.1155/2021/6630236

[58] Bogaard, R.H. (1985). Thermal Conductivity of Selected Stainless Steels . In: *Thermal Conductivity 18* (Eds. Ashworth, T., Smith, D.R.), pp. 175–185, Springer, Boston, MA. doi: 10.1007/978-1-4684-4916-7_20

[59] Bentz, D.P., & Prasad, K.R. (2007). *Thermal performance of fire restrictive materials I. characterization with respect to thermal performance models*. National Institute of Standards Technology IR 7401. doi: 10.6028/nist.ir.7401

[60] Assael, M.J., Gialou, K., Kakosimos, K., & Metaxa, I. (2004). Thermal Conductivity of Reference Solid Materials. *International Journal of Thermophysics*, 25(2), 397–408. doi: 10.1023/b:ijot.0000028477.74595.d5

[61] Tang, B., Zhu, C., Xu, M., Chen, T., & Hu, S. (2019). Thermal conductivity of sedimentary rocks in the Sichuan Basin, Southwest China. *Energy Exploration & Exploitation*, 37(2), 691–720. doi: 10.1177/0144598718804902

[62] Halbert, D., & Parnell, J. (2022). Thermal conductivity of basalt between 225 and 290 K. *Meteoritics & Planetary Science*, 57(8), 1617–1626. doi: 10.1111/maps.13829

[63] Joint Committee for Guides in Metrology. (2008). *Evaluation of measurement data — Guide to the expression of uncertainty in measurement*, JCGM 100:2008.